

Heavy-flavor effects in soft gluon resummation for electroweak boson production at hadron colliders

Stefan Berge,^{1*} Pavel M. Nadolsky,^{2†} and Fredrick I. Olness,^{1‡}

¹*Department of Physics,*

Southern Methodist University,

Dallas, Texas 75275-0175, U.S.A.

²*High Energy Physics Division,*

Argonne National Laboratory,

Argonne, IL 60439-4815, U.S.A.

(Dated: 1st May 2018)

Abstract

We evaluate the impact of heavy-quark masses on transverse momentum (q_T) distributions of W , Z , and supersymmetric neutral Higgs bosons at the Tevatron and LHC. The masses of charm and bottom quarks act as non-negligible momentum scales at small q_T and affect resummation of soft and collinear radiation. We point out inconsistencies in the treatment of heavy-flavor channels at small q_T in massless and fixed-flavor number factorization schemes, and formulate small- q_T resummation in a general-mass variable flavor number factorization scheme. The improved treatment of the quark mass dependence leads to non-negligible effects in precision measurements of the W boson mass at the LHC and may cause observable modifications in production of Higgs bosons and other particles in heavy-quark scattering.

PACS numbers: 12.15.Ji, 12.38 Cy, 13.85.Qk

* E-mail: berge@mail.physics.smu.edu

† E-mail: nadolsky@hep.anl.gov

‡ E-mail: olness@smu.edu

I. INTRODUCTION

Key electroweak observables of the standard model (SM), such as the mass and width of W bosons, will be measured with high precision in production of W^\pm and Z^0 bosons in hadron collisions at the Fermilab (Tevatron) and Large Hadron Collider at CERN (LHC). The uncertainty in the W boson mass M_W will be reduced to 30-40 MeV per experiment in the Tevatron Run-2 and to about 15 MeV at the LHC [1, 2]. At this level of accuracy, the theory framework must incorporate effects were dismissed in less precise analyses.

One such feature is the dependence on masses of quarks, which is frequently neglected in hard-scattering reactions. While the massless approximation is clearly appropriate in channels involving only light quarks (u , d , and perhaps s), it may be less adequate when heavy quarks (c and b) are involved, particularly when the cross section depends on a small momentum scale close to the mass m_Q of the heavy quark. The distributions of heavy electroweak bosons over their transverse momenta q_T may be sensitive to the masses of c and b quarks, given that the transverse momenta of most bosons (of order, or less than a few GeV) are comparable to m_Q . The impact of the quark masses on the q_T distributions of bosons with invariant masses $Q \geq M_W$ is suppressed by properties of soft parton radiation, as demonstrated below. Nonetheless, the quark mass effects are relevant in high-precision studies, such as the measurement of M_W , or in reactions dominated by scattering of heavy quarks (particularly bottom quarks), such as Higgs boson production in $b\bar{b}$ annihilation.

In the present paper, we quantify the effects of the heavy-quark masses on q_T distributions in Drell-Yan production of W^\pm , Z^0 , and Higgs bosons. We evaluate the associated impact on the W boson mass measurement and demonstrate the importance of the quark-mass corrections in the processes initiated by bottom quarks, like $b\bar{b} \rightarrow \text{Higgs}$. This latter channel can have a large cross section in supersymmetric extensions of the standard model [3, 4, 5].

The description of the heavy-quark scattering is complex because of the presence of the heavy-quark mass scale m_Q , in addition to the boson's transverse momentum q_T and its virtuality Q . Two popular factorization schemes (fixed-flavor number (FFN) scheme [6, 7, 8, 9, 10, 11] and zero-mass variable flavor number (ZM-VFN) scheme) were applied recently to calculate various observables in the b -quark channels [12, 13, 14, 15, 16, 17, 18, 19, 20]. However, neither of the two schemes is entirely consistent when describing logarithmic corrections in processes like $b\bar{b} \rightarrow H$ in the small- q_T region. When q_T is much smaller than Q , the calcula-

tion of the q_T distribution in perturbative quantum chromodynamics (PQCD) must evaluate an all-order sum of large logarithms $\ln(q_T^2/Q^2)$, arising as a consequence of the recoil of the electroweak bosons against unobserved hadrons of relatively low energy or transverse momentum (soft and collinear hadrons). The resummation of Drell-Yan q_T distributions for massless initial-state quarks has been developed in a variety of forms [21, 22, 23, 24, 25, 26, 27]. In the present paper we use the Collins-Soper-Sterman formalism (CSS) [24], which excellently describes the available q_T data from fixed-target Drell-Yan experiments and Z^0 boson production at the Tevatron. When applied to heavy-quark scattering, small- q_T resummation indispensably involves logarithms depending on both the transverse momentum, $\ln(q_T^2/Q^2)$, and heavy-quark mass, $\ln(\mu_F^2/m_Q^2)$. To correctly treat both types of large contributions, Ref. [28] extended the CSS formalism to a general-mass variable flavor number (GM-VFN) scheme [29]. The extended resummation formalism was then applied to describe heavy-flavor production in deep inelastic scattering (DIS). We review the q_T resummation formalism for heavy quarks in Section II.

The present study was motivated by the results of Ref. [28], where the correct treatment of the heavy-quark masses was found to substantially change the differential cross sections for heavy quark production in DIS at small $q_T \approx m_Q$. In Section III, we extend that study to examine the heavy-flavor effects on q_T distributions of W^\pm , Z^0 , and Higgs bosons produced at the Tevatron and LHC. To get a first idea about the magnitude of the mass effects, we consider fractional contributions of reaction channels with initial-state c and b quarks to the entire production rate (see Table I). At the Tevatron, the heavy-quark channels contribute only 8% (3%) of the inclusive cross section in W^\pm (Z^0) boson production, and consequently the quark masses can be usually neglected. At the LHC, the heavy-quark channels add up to 22% in W^+ and 31% in W^- boson production. Modifications caused by the heavy-quark masses at the LHC are comparable to the other uncertainties and must be considered in precision measurements of M_W . We then turn to Higgs boson production in the $b\bar{b} \rightarrow H$ channel. We show that the nonzero mass of the bottom quark substantially modifies the small- q_T Higgs distribution. Furthermore, we note that other processes with initial-state heavy quarks, like $bg \rightarrow Z^0b$, H^-t , $H^+\bar{t}$, H^0b , etc. will be affected by the heavy-quark masses in a similar way. We summarize the results of this study in Section IV.

II. TRANSVERSE MOMENTUM RESUMMATION FOR MASSIVE QUARKS

A. General form of the resummed form factor

In this section, we define the essential elements for the transverse momentum resummation in the presence of massive quarks. The resummed differential cross section for the inclusive production of heavy electroweak bosons in scattering of initial-state hadrons A and B takes the form [24]

$$\frac{d\sigma}{dQ^2 dy dq_T^2} = \int_0^\infty \frac{bdb}{2\pi} J_0(q_T b) \widetilde{W}(b, Q, x_A, x_B, \{m_Q\}) + Y(q_T, Q, y, \{m_Q\}), \quad (1)$$

where $y = (1/2) \ln [(E + p_z)/(E - p_z)]$ is the rapidity of the vector boson, $x_{A,B} \equiv Q e^{\pm y} / \sqrt{S}$ are the Born-level partonic momentum fractions, S is the square of the center-of-mass energy of the collider, and $J_0(q_T b)$ is the Bessel function. The integral is the Fourier-Bessel transform of a form factor $\widetilde{W}(b, Q, x_A, x_B, \{m_Q\})$ in impact parameter (b) space, which contains the all-order sum of the logarithms $\alpha_s^n \ln^m(q_T^2/Q^2)$. The b -space form factor is given by

$$\widetilde{W}(b, Q, x_A, x_B, \{m_Q\}) = \frac{\pi}{S} \sum_{j,k} \sigma_{jk}^{(0)} e^{-\mathcal{S}(b, Q, \{m_Q\})} \overline{\mathcal{P}}_{j/A}(x_A, b, \{m_Q\}) \overline{\mathcal{P}}_{k/B}(x_B, b, \{m_Q\}), \quad (2)$$

where the summation is performed over the relevant parton flavors j and k . Here, $\sigma_{jk}^{(0)}$ is the product of the Born-level prefactors, $e^{-\mathcal{S}(b, Q, \{m_Q\})}$ is an exponential of the Sudakov integral

$$\mathcal{S}(b, Q, \{m_Q\}) \equiv \int_{b_0^2/b^2}^{Q^2} \frac{d\bar{\mu}^2}{\bar{\mu}^2} \left[\mathcal{A}(\alpha_s(\bar{\mu}), \{m_Q\}) \ln\left(\frac{Q^2}{\bar{\mu}^2}\right) + \mathcal{B}(\alpha_s(\bar{\mu}), \{m_Q\}) \right], \quad (3)$$

and $\overline{\mathcal{P}}_{j/A}(x, b, \{m_Q\})$ are the b -dependent parton distributions. The constant factor $b_0 \equiv 2e^{-\gamma_E} \approx 1.123$ appears in several places when a momentum scale is constructed from the impact parameter, as in the lower limit b_0^2/b^2 of integration in Eq. (3). The Sudakov exponential and b -dependent parton densities resum contributions from soft and collinear multi-parton radiation, respectively. In the perturbative region ($b^2 \ll \Lambda_{QCD}^{-2}$), the distributions $\overline{\mathcal{P}}_{j/A}(x, b, \{m_Q\})$ factorize as

$$\begin{aligned} \overline{\mathcal{P}}_{j/A}(x, b, \{m_Q\})|_{b^2 \ll \Lambda_{QCD}^{-2}} &= \sum_{a=g,u,d,\dots} \int_x^1 \frac{d\xi}{\xi} \mathcal{C}_{j/a}(x/\xi, b, \{m_Q\}, \mu_F) f_{a/A}(\xi, \mu_F) \\ &\equiv (\mathcal{C}_{j/a} \otimes f_{a/A})(x, b, \{m_Q\}, \mu_F) \end{aligned} \quad (4)$$

into a sum of convolutions of the Wilson coefficient functions $\mathcal{C}_{j/a}(x, b, \{m_Q\}, \mu_F)$ and k_T -integrated parton distributions $f_{a/A}(\xi, \mu_F)$. Note that the initial state A can be a hadron as well as a parton, in which case we denote the partonic initial state as A' .

If quark masses $\{m_{\mathcal{Q}}\}$ are neglected in the coefficient function $\mathcal{C}_{j/a}(x, b, \{m_{\mathcal{Q}}\}, \mu_F)$, it depends on b and μ_F only through the logarithm $\ln(\mu_F b/b_0)$:

$$\lim_{\{bm_{\mathcal{Q}}\} \rightarrow \{0\}} \mathcal{C}_{j/a}(x, b, \{m_{\mathcal{Q}}\}, \mu_F) = \mathcal{C}_{j/a}(x, \ln \frac{b\mu_F}{b_0}). \quad (5)$$

For this reason, we set the factorization scale μ_F equal to b_0/b to prevent the large logarithms $\ln(\mu_F b/b_0)$ from appearing in $\mathcal{C}_{j/a}$ in the limit $b \rightarrow 0$.

$Y(q_T, Q, y, \{m_{\mathcal{Q}}\})$ in Eq. (1) is the regular part, defined as the difference of the fixed-order cross section and the expansion of the Fourier-Bessel integral to the same order of α_s ; it dominates at $q_T \sim Q$ and is small at $q_T \rightarrow 0$. The regular piece Y and the dominant contributions in \widetilde{W} can be calculated in PQCD, if Q is sufficiently large. A small nonperturbative component in \widetilde{W} contributing at q_T less than a few GeV can be approximated within one of the available models. Our specific choice of the nonperturbative model is described in Section II C.

B. Extension to the case of massive quarks

Eqs. (1) and (2) indicate that \widetilde{W} and Y may explicitly depend on the masses of heavy quarks $\{m_{\mathcal{Q}}\}$, with $\mathcal{Q} = c, b$, and t . Masses of the light u, d , and s quarks ($m_{u,d,s} \lesssim \Lambda_{QCD}$) are neglected by definition in hard-scattering contributions and implicitly retained in the nonperturbative functions, *i.e.*, parton densities $f_{a/A}(x, \mu_F)$ and power corrections to \widetilde{W} at large impact parameters $b > 1 \text{ GeV}^{-1}$. Indeed, the nonperturbative dynamics described by $f_{a/A}(x, \mu_F)$ and power corrections does depend on the light-quark masses, but this dependence is not separated explicitly from the other nonperturbative effects.

In contrast to the masses of u, d , and s quarks, masses of the heavy quarks must be retained in the hard-scattering terms in some cases. Several viable options exist for the treatment of $\{m_{\mathcal{Q}}\}$, depending on the energy and flavor composition of the scattering reaction. In two common approaches, the heavy quark contributions to the PDF's $f_{a/A}(x, \mu_F)$ and other resummed functions are either neglected or, alternatively, treated on the same footing as contributions from the light quarks (u, d , and s) above the respective heavy-quark mass thresholds, often placed, for convenience, at $\mu_F = m_{\mathcal{Q}}$. These choices correspond to the FFN and ZM-VFN factorization schemes, respectively. The FFN scheme optimally organizes the perturbative QCD series at energies of order of the heavy-quark mass $m_{\mathcal{Q}}$.

The ZM-VFN scheme is the best choice for inclusive (depending on one momentum scale) distributions at energies much larger than m_Q . It commonly utilizes dimensional regularization to expose collinear singularities of massless partonic matrix elements as $1/\epsilon^p$ poles in $n = 4 - 2\epsilon$ dimensions.

Neither of the two schemes is entirely satisfactory when applied to differential distributions depending on two or more momentum scales of distinct magnitudes, as is the case of small- q_T resummation at large Q . At sufficiently large \sqrt{S} , the heavy-flavor quarks are copiously produced by quasi-collinear splittings of gluons along the directions of the initial-state hadrons. Such collinear contributions must be resummed at $Q \gg m_Q$ in the parton density $f_{Q/A}(x, \mu_F)$ for the heavy quarks Q , so that a VFN factorization scheme is needed. If all scales (including q_T) are of order Q , the heavy-quark mass $m_Q \ll q_T \sim Q$ can be neglected in the hard-scattering matrix elements, reducing the result to the ZM-VFN scheme. But m_Q cannot be omitted at small q_T ($m_Q \sim q_T \ll Q$), where it is not small compared to the momentum of the soft and collinear radiation.

In b -space, the form factor $\widetilde{W}(b, Q, x_A, x_B, \{m_Q\})$ is not well-defined in the ZM-VFN scheme in the heavy-quark channels at impact parameters $b > b_0/m_Q$, corresponding to factorization scales μ_F below the heavy-quark mass threshold, $\mu_F = b_0/b < m_Q$. For charm quarks with mass $m_c = 1.3$ GeV and bottom quarks with mass $m_b = 4.5$ GeV, the ZM-VFN form factor \widetilde{W} is not well-defined at $b > 0.86$ and 0.25 GeV $^{-1}$, respectively. The problem lies with the heavy-quark Wilson coefficient function $\mathcal{C}_{Q/A}(x, b, m_Q, \mu_F)$, which is derived by using the factorization relation of Eq. (4) with the densities $\overline{\mathcal{P}}_{Q/A'}(x, b, m_Q)$ and $f_{a/A'}(x, \mu_F)$ of heavy quarks in partonic initial states $A' = q, Q, g$. At μ_F below the threshold, the k_T -integrated heavy-quark density $f_{Q/A'}(x, \mu_F)$ is set identically equal to zero, in accordance with the definition of $f_{Q/A'}(x, \mu_F)$ in the ZM-VFN scheme. Consequently the collinear poles $1/\epsilon$ arising in the calculation of the b -dependent density $\overline{\mathcal{P}}_{Q/A'}(x, b)$ for massless splittings $Q \leftarrow A'$ in $n \neq 4$ dimensions cannot be canceled by $f_{a/A'}(x, \mu_F)$ at such μ_F . Eq. (4) then implies that the Wilson coefficient function $\mathcal{C}_{Q/A}(x, b, m_Q, \mu_F)$ may be also infinite (contain the $1/\epsilon$ poles) below the heavy-quark threshold. The infinity arises because the ZM-VFN scheme incorrectly neglects the heavy-quark mass m_Q at energies $\mu_F = b_0/b$ of order or less than m_Q . The solution to this problem is to retain the dependence on m_Q at $b \gtrsim b_0/m_Q$, which can be realized by formulating the CSS resummation in the GM-VFN factorization scheme.

The GM-VFN scheme [29] consistently implements the heavy-quark masses at all energy scales μ_F , and it reproduces the FFN and ZM-VFN schemes in the limits $\mu_F \lesssim m_Q$ and $\mu_F \gg m_Q$, respectively. Several versions of the GM-VFN scheme have been developed in the past years [30, 31, 32, 33, 34, 35, 36, 37, 38]. A general procedure for the implementation of the GM-VFN scheme in q_T resummation was outlined in Ref. [28], where an application of the CSS resummation in the simplified Aivazis-Collins-Olness-Tung (S-ACOT) factorization scheme [29, 37] was presented for production of heavy quarks at HERA.

The S-ACOT scheme is a variant of the GM-VFN scheme, which simplifies computations by neglecting the heavy-quark masses in hard subgraphs with incoming heavy quarks (flavor-excitation graphs), such as $\mathcal{Q} + g \rightarrow \mathcal{Q} + g$. The heavy-quark masses are retained in the hard subgraphs with explicit production of heavy quarks (flavor-creation graphs), such as $g + g \rightarrow \mathcal{Q} + \bar{\mathcal{Q}}$. As demonstrated in Ref. [28], application of the S-ACOT rules to the CSS resummed cross section efficiently retains the dependence on the heavy-quark masses where it is important, and drops it where it is not essential.

In production of heavy gauge bosons ($Q \gg m_Q$), the S-ACOT rules allow us to drop the m_Q dependence at $q_T \gg m_Q$ and keep the essential m_Q dependence at $q_T \lesssim m_Q$. We assume that the heavy quarks are pairwise produced in perturbative splittings of gluons. We neglect possible, but yet experimentally unconfirmed, nonperturbative “intrinsic” heavy-quark contributions to the proton wavefunction [39]. We neglect the mass dependence entirely in the Y -term, as it is non-negligible only at $q_T \gg m_Q$. In the \widetilde{W} -term, we drop the m_Q dependence in all flavor-excitation hard subgraphs and keep it in all flavor-creation hard subgraphs. By this rule, m_Q is dropped in the perturbative Sudakov form factor \mathcal{S} and the coefficient functions $\mathcal{C}_{a/\mathcal{Q}}$ with the incoming heavy quarks, both of which are described by the flavor-excitation Feynman graphs. We evaluate \mathcal{S} up to $\mathcal{O}(\alpha_s^2/\pi^2)$ and $\mathcal{C}_{a/\mathcal{Q}}$ up to $\mathcal{O}(\alpha_s/\pi)$ by using their massless expressions.

We keep the m_Q dependence in the gluon-initiated coefficient functions $\mathcal{C}_{\mathcal{Q}/g}$, since those are computed from the flavor-creation Feynman graphs. The mass-dependent $\mathcal{O}(\alpha_s/\pi)$ coefficient $\mathcal{C}_{\mathcal{Q}/g}^{(1)}$ in $\mathcal{C}_{\mathcal{Q}/g}$ is given by [28]

$$\begin{aligned} \mathcal{C}_{\mathcal{Q}/g}^{(1)}(x, b, m_Q, \mu_F) &= T_R x (1-x) b m_Q K_1(b m_Q) \\ &\quad + P_{q/g}^{(1)}(x) \left[K_0(b m_Q) - \theta(\mu_F - m_Q) \ln\left(\frac{\mu_F}{m_Q}\right) \right], \end{aligned} \quad (6)$$

where $P_{q/g}^{(1)}(x) = T_R [x^2 + (1-x)^2]$ is the $q \leftarrow g$ splitting function, $T_R = 1/2$, and $K_0(z)$ and

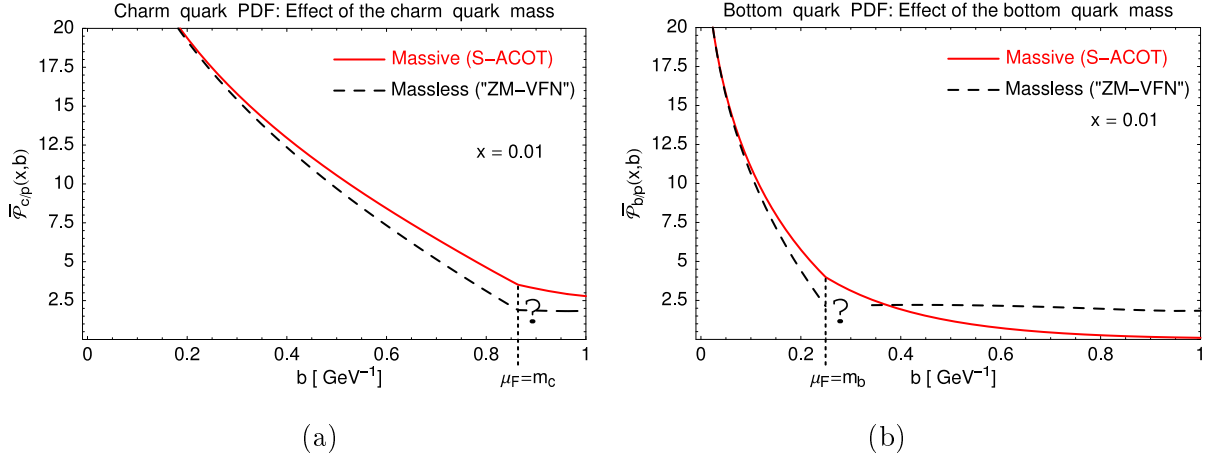


Figure 1: The b -dependent parton densities $\bar{P}_{Q/A}(x, b, m_Q)$ vs. the impact parameter b for (a) charm quarks and (b) bottom quarks. The solid and dashed curves correspond to the S-ACOT and massless (“ZM-VFN”) factorization schemes, respectively.

$K_1(z)$ are the modified Bessel functions [40]. The term proportional to the step function $\theta(\mu_F - m_Q)$ is nonzero above the heavy-quark threshold ($\mu_F \geq m_Q$), where the collinear logarithm $P_{q/g}^{(1)}(x) \ln(\mu_F/m_Q)$ is subtracted from $\mathcal{C}_{Q/g}^{(1)}(x, b, m_Q, \mu_F)$ and absorbed into the heavy-quark PDF $f_{Q/A}(x, \mu_F)$. The subtraction is not performed below the heavy-quark threshold, because $f_{Q/A}(x, \mu_F) = 0$ at $\mu_F < m_Q$. For $b m_Q \ll 1$, the gluon-initiated coefficient function reduces to its massless expression,

$$\lim_{b m_Q \rightarrow 0} \mathcal{C}_{Q/g}^{(1)}(x, b, m_Q, \mu_F) = T_R x (1 - x) - P_{q/g}^{(1)}(x) \ln(\mu_F b / b_0). \quad (7)$$

Convolutions of the Wilson coefficient functions $\mathcal{C}_{Q/A}(x, b, m_Q, \mu_F)$ and k_T -integrated PDF’s $f_{a/A}(x, \mu_F)$ are combined into the b -dependent parton density $\bar{P}_{Q/A}(x, b, m_Q)$ according to Eq. (4). At an n -th order of α_s , $\bar{P}_{Q/A}(x, b, m_Q)$ and its derivatives are continuous in $\ln(b)$ up to order n , if computed in the S-ACOT scheme. Here the order of $\bar{P}_{Q/A}(x, b, m_Q)$ is determined by a formal counting of powers of α_s appearing both in the coefficient functions and PDF’s. In this counting, the PDF $f_{Q/A'}(x, \mu_F)$ for perturbatively generated heavy quarks is one order higher in α_s than the light-parton PDF’s.

At leading order (LO), the function $\bar{P}_{Q/A}(x, b, m_Q)$ is composed of the heavy-quark-initiated coefficient function $\mathcal{C}_{Q/Q}(x, b, m_Q, \mu_F)$, evaluated at order α_s^0 , and the gluon coefficient function $\mathcal{C}_{Q/g}(x, b, m_Q, \mu_F)$, evaluated at order α_s/π :

$$\bar{P}_{Q/A}(x, b, m_Q) = \left(\mathcal{C}_{Q/Q}^{(0)} \otimes f_{Q/A} \right) (x, b, m_Q, \mu_F)$$

$$+ \frac{\alpha_s(\mu_F)}{\pi} \left(\mathcal{C}_{Q/g}^{(1)} \otimes f_{g/A} \right) (x, b, m_Q, \mu_F) + \mathcal{O}(\alpha_s^2/\pi^2). \quad (8)$$

Here $\mathcal{C}_{Q/Q}^{(0)}(x, b, m_Q, \mu_F) = \delta(1 - x)$. The dependence of the leading-order (LO) parton density $\bar{\mathcal{P}}_{Q/A}(x, b, m_Q)$ on b is shown for the charm quarks in Fig. 1(a) and bottom quarks in Fig. 1(b). The factorization scale μ_F is set equal to b_0/b to correctly resum the collinear logarithms in $f_{Q/A}(x, \mu_F)$ in the small- b limit (cf. Eq. (5)). Together with the S-ACOT predictions (solid lines), we show the ZM-VFN predictions (dashed lines).

As discussed above, the ZM-VFN parton density $\bar{\mathcal{P}}_{Q/A}(x, b, m_Q)$ is not properly defined below the threshold $\mu_F = m_Q$ (or above $b = b_0/m_Q$). We formally define the “ZM-VFN” density $\bar{\mathcal{P}}_{Q/A}(x, b, m_Q)$ at $b > b_0/m_Q$ according to Eq. (8) by using massless Wilson coefficient functions $\mathcal{C}_{j/a}(x, b, m_Q = 0, \mu_F)$, as it was done in the previous resummation calculations. Such a definition provides just one of many possible continuations of the “ZM-VFN” coefficient functions below the heavy-quark threshold, which render different results in q_T space. We indicate this ambiguity by enclosing “ZM-VFN” in quotes and placing a question mark by the dashed line in Fig. 1. At $b > b_0/m_Q$, the first term on the right-hand side of Eq. (8) vanishes ($f_{Q/A}(x, \mu_F) = 0$), so that $\bar{\mathcal{P}}_{Q/A}(x, b, m_Q)$ becomes equal to the second term:

”ZM-VFN”, $b > b_0/m_Q$:

$$\bar{\mathcal{P}}_{Q/A}(x, b, m_Q = 0) = \frac{\alpha_s(\mu_F)}{\pi} \left(\mathcal{C}_{Q/g}^{(1)} \otimes f_{g/A} \right) (x, b, m_Q = 0, \mu_F) + \mathcal{O}(\alpha_s^2/\pi^2). \quad (9)$$

The massless $Q \leftarrow g$ coefficient function $\mathcal{C}_{Q/g}(x, b, m_Q = 0, \mu_F)$ in Eq. (9) is given by Eq. (7).

As in the ZM-VFN scheme, the heavy-quark PDF $f_{Q/A}(x, \mu_F)$ vanishes below the heavy-quark threshold in the S-ACOT scheme. However, the S-ACOT scheme properly preserves the mass-dependent terms below the threshold as a part of the gluon-initiated coefficient function $\mathcal{C}_{Q/g}^{(1)}(x, b, m_Q, \mu_F)$. The S-ACOT parton density $\bar{\mathcal{P}}_{Q/A}(x, b, m_Q)$ is well-defined at all b . It reduces to the ZM-VFN result at $b \ll b_0/m_Q$ and is strongly suppressed at $b \gg b_0/m_Q$ by the modified Bessel functions $K_0(b m_Q)$ and $K_1(b m_Q)$. The large- b suppression is particularly strong in the case of the bottom quarks, where $\bar{\mathcal{P}}_{b/p}(x, b, m_b)$ is essentially negligible at $b > 1 \text{ GeV}^{-1}$ (cf. Fig. 1b). The suppression is caused by the decoupling of the heavy quarks in the parton densities at μ_F much smaller than m_Q (b much larger than b_0/m_Q). This suppression is independent from the suppression of contributions with $b \gtrsim 0.5 - 1 \text{ GeV}^{-1}$ by the Sudakov exponential $e^{-\mathcal{S}(b, Q)}$ (see Section II D), and it does not depend on Q . Consequently the impact of the nonperturbative contributions from $b \gtrsim 1 \text{ GeV}^{-1}$ is reduced in the heavy-quark channels comparatively to the light-quark channels.

C. Nonperturbative contributions

To gauge the effect of the nonperturbative contributions on the form factor \widetilde{W} , we must estimate the behavior of the Sudakov exponential $e^{-\mathcal{S}(b,Q)}$ and b -dependent parton densities $\overline{\mathcal{P}}_{j/A}(x, b, \{m_Q\})$ at large b . Many studies have investigated the nonperturbative contributions to the resummed form factor; see, e.g., Refs. [24, 26, 27, 41, 42, 43, 44, 45, 46, 47, 48, 49]. Here we opt to use a new parameterization of the nonperturbative component found in a global analysis [50] of Drell-Yan pair and Z boson production. This parameterization is obtained in the revised b_* model [24, 51], with the free model parameters chosen as to maximally preserve the exact form of the perturbative contributions at $b < 1 \text{ GeV}^{-1}$ [50].

The b_* model introduces a function $b_*(b, b_{max}) \equiv b/\sqrt{1+b^2/b_{max}^2}$ and defines the resummed form factor \widetilde{W} as

$$\widetilde{W}(b, Q, x_A, x_B, \{m_Q\}) \equiv \widetilde{W}_{pert}(b_*(b, b_{max}), Q, x_A, x_B, \{m_Q\}) e^{-\mathcal{F}_{NP}(b, Q)} \quad (10)$$

at all b , with $\widetilde{W}_{pert}(b_*(b, b_{max}), Q, x_A, x_B, \{m_Q\})$ being the finite-order (“perturbative”) approximation to $\widetilde{W}(b, Q, x_A, x_B, \{m_Q\})$. The higher-order corrections in α_s and “powersuppressed” terms proportional to positive powers of b are cumulatively described by the nonperturbative function $\mathcal{F}_{NP}(b, Q)$, defined as

$$\mathcal{F}_{NP}(b, Q) \equiv -\ln \left(\frac{\widetilde{W}(b, Q, x_A, x_B, \{m_Q\})}{\widetilde{W}_{pert}(b_*(b, b_{max}), Q, x_A, x_B, \{m_Q\})} \right)$$

and found by fitting to the data.

In accordance with Ref. [50], we choose $b_{max} = 1.5 \text{ GeV}^{-1}$. We also choose the factorization scale μ_F in $(\mathcal{C} \otimes f)(x, b, \{m_Q\}, \mu_F)$ such that it stays above the initial scale $Q_0 \sim 1 \text{ GeV}$ for the PDF’s $f_{a/A}(x, \mu_F)$. Specifically, we define $\mu_F \equiv b_0/b_*(b, b_0/Q_0) = (Q_0^2 + b_0^2/b^2)^{1/2}$, so that μ_F is approximately equal to b_0/b at $b \rightarrow 0$ and asymptotically approaches Q_0 at $b \rightarrow \infty$.

The function $\mathcal{F}_{NP}(b, Q)$ found in the fit of Ref. [50] has the form

$$\mathcal{F}_{NP}(b, Q) \equiv b^2 [0.201 + 0.184 \ln(Q/(3.2 \text{ GeV})) - 0.026 \ln(100 x_A x_B)]. \quad (11)$$

This parameterization has several advantages compared to the previous nonperturbative models. First, it minimizes modifications in $\widetilde{W}_{pert}(b, Q, x_A, x_B, \{m_Q\})$ by the b_* prescription in the small- b region, where perturbation theory is valid. Second, Eq. (11) is in a good

agreement with both the available q_T data and theoretical expectations. $\mathcal{F}_{NP}(b, Q)$ has a quadratic form, $\mathcal{F}_{NP} \propto b^2$, and follows a nearly linear dependence on $\ln(Q)$, which can be seen in Eq. (11) if the small term $-0.026 \ln(100 x_A x_B)$ is neglected. The quadratic form leads to Gaussian smearing by nonperturbative “intrinsic- k_T ” effects: $\widetilde{W}(b, Q) \sim e^{-0.5 \langle k_T^2 \rangle b^2}$, with $\langle k_T^2 \rangle \lesssim 1 \text{ GeV}^2$ in the observable Q range. Both the quadratic form and linear $\ln(Q)$ dependence of $\mathcal{F}_{NP}(b, Q)$ are suggested by the infrared renormalon analysis of the large- b contributions [52]. The coefficient $a_2 = 0.184 \text{ GeV}^2$ of the $\ln(Q)$ term (found in the fit) agrees well with its independent estimate $0.19_{-0.09}^{+0.12} \text{ GeV}^2$ obtained within the renormalon analysis [53]. The $\ln(Q)$ term arises from the Sudakov factor as a consequence of the renormalization-group invariance of the resummed form factor [51]. It does not depend on the quark flavors, and it contributes about 70% to the magnitude of $\mathcal{F}_{NP}(b, Q)$ at $Q \sim M_Z$. Therefore, we expect the large flavor-independent term $0.184 b^2 \ln(Q/3.2 \text{ GeV})$ to be also present in the heavy-quark scattering channels.

The other terms in Eq. (11) may in principle depend on the flavor of the participating quarks. However, no obvious dependence on the quark flavor or nucleon isospin was observed in the global q_T fit to the Drell-Yan pair and Z boson production data [50], perhaps because these data are mostly sensitive to the scattering of light u and d quarks. Additional nonperturbative contributions may be present in the heavy-quark sector, especially if the “intrinsic” heavy-quark states [39] constitute a non-negligible part of the proton’s wavefunction. In the classical realization, the intrinsic heavy quarks contribute at large momentum fractions ($x \rightarrow 1$), while the bulk of W and Z boson production happens at much smaller x , $x = 10^{-3} - 10^{-1}$. Since the existence of the “intrinsic” heavy quarks remains an open question, we do not consider them in this study. We therefore parametrize the nonperturbative contributions by Eq. (11), which neglects the flavor dependence. We vary the parameters of $\mathcal{F}_{NP}(b, Q)$ in the heavy-quark channels in order to evaluate the uncertainty in the physical observables arising from this approximation.

D. An example of the b -space form factor

Fig. 2 shows an example of the full resummed form factor $b \widetilde{W}(b, Q)$ (cf. Eq. (2)) in Z boson production via $b\bar{b}$ annihilation in the Tevatron Run-2. The form factor is computed in the S-ACOT scheme at the leading-order (LO) and in the S-ACOT and

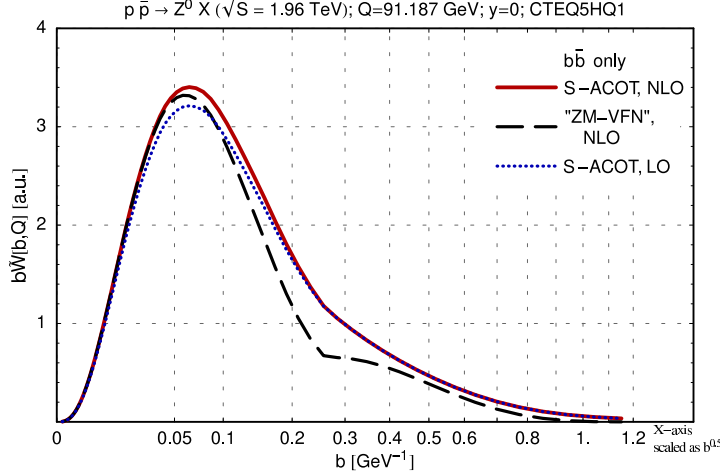


Figure 2: The form factor $b\tilde{W}(b, Q)$ vs. the impact parameter b for $b\bar{b} \rightarrow Z^0 X$ in the Tevatron Run-2. The solid, dashed, an dotted curves correspond to the NLO S-ACOT, NLO “ZM-VFN”, and LO S-ACOT calculations, respectively.

“ZM-VFN” schemes at the partial next-to-leading-order (NLO). The leading-order “ZM-VFN” contribution is computed by using the formal definition of $\bar{\mathcal{P}}_{Q/A}(x, b, m_Q = 0)$ in Eq. (8). The NLO curves are obtained by adding the massless flavor-excitation contribution $(\mathcal{C}_{Q/Q}^{(1)} \otimes f_{Q/A})(x, b, m_Q = 0, \mu_F)$ of order $\mathcal{O}(\alpha_s/\pi)$ to the LO parton density $\bar{\mathcal{P}}_{Q/A}(x, b, m_Q)$ in Eq. (8). We do not include the $\mathcal{O}(\alpha_s^2/\pi^2)$ flavor-creation contribution $(\mathcal{C}_{Q/a}^{(2)} \otimes f_{a/A})(x, b, m_Q, \mu_F)$, with $a = q, g$, needed to evaluate $\bar{\mathcal{P}}_{Q/A}(x, b, \{m_Q\})$ at the full NLO accuracy. The partial NLO approximation results in a discontinuity of the derivative $d\tilde{W}(b, Q)/d\ln b$ at the bottom quark threshold, which has little impact on our results. The perturbative contribution to the Sudakov factor $\mathcal{S}(b, Q)$ is evaluated up to order α_s^2/π^2 . The nonperturbative terms are included according to Eqs. (10) and (11), assuming flavor independence of $\mathcal{F}_{NP}(b, Q)$. Furthermore, the CTEQ5HQ1 parton distributions [54] were used.

According to the figure, the form factor $b\tilde{W}(b, Q)$ in $b\bar{b} \rightarrow Z$ exhibits a maximum at $b \approx 0.07 \text{ GeV}^{-1}$. Larger impact parameters are suppressed by the Sudakov exponential $e^{-\mathcal{S}(b, Q)}$ by an amount growing with Q , independently of the quark flavor and factorization scheme. In the S-ACOT scheme, the form factor is also suppressed by the m_Q decoupling in $\bar{\mathcal{P}}_{Q/A}(x, b, m_Q)$. Consequently the mass-dependent variations in $b\tilde{W}(b, Q)$ are more pronounced in production of not too heavy bosons, such as Z^0 , and in bottom quark channels, where they occur at relatively small $b \approx 0.25 \text{ GeV}^{-1}$ (cf. Fig. 1).

The “ZM-VFN” form factor underestimates the S-ACOT form factor in a wide range of b , and it exhibits non-smooth behavior in the vicinity of the bottom quark threshold. The NLO S-ACOT and “ZM-VFN” form factors agree well at $b < 0.05$ GeV $^{-1}$. The NLO correction to $\bar{\mathcal{P}}_{Q/A}(x, b, m_Q)$ mainly contributes at $b \approx 0.02 - 0.25$ GeV $^{-1}$, where it enhances the LO form factor. The NLO correction is turned off at $b > 0.25$ GeV $^{-1}$ by the condition $f_{Q/A}(x, \mu_F) = 0$ for $\mu_F < m_Q$. It is also suppressed at $b < 0.02$ GeV $^{-1}$ by the small $\alpha_s(b_0/b)$.

The differences between the S-ACOT and “ZM-VFN” form factors seen at $b \approx b_0/m_Q$ will affect the cross sections in q_T space at small and moderate transverse momenta.

III. NUMERICAL RESULTS

In the present section we compare the resummed q_T distributions calculated in the massive (S-ACOT) and massless (“ZM-VFN”) schemes, defined according to Eq. (9). We examine Drell-Yan production of W^\pm , Z^0 , and Higgs bosons in the Tevatron Run-2 (the c.m. energy $\sqrt{S} = 1.96$ TeV) and at the LHC ($\sqrt{S} = 14$ TeV). In the case of W boson production, we consider the leptonic decay mode $W \rightarrow e\nu$ and discuss the impact of the different schemes on the measurement of the W boson mass. We apply the resummation formalism described in the previous section. The numerical calculation was performed using the programs Legacy and ResBos [48, 55] with the CTEQ5HQ1 parton distribution functions [54]. We use the parameterization (11) for the nonperturbative function $\mathcal{F}_{NP}(b, Q)$, unless stated otherwise. The W^\pm and Z^0 boson masses are assumed to be $M_W = 80.423$ GeV and $M_Z = 91.187$ GeV, respectively. The heavy quark masses are taken to be $m_c = 1.3$ GeV and $m_b = 4.5$ GeV.

A. Partonic subprocesses in W^\pm and Z^0 boson production

We first compare contributions of various partonic subprocesses to the total W^\pm and Z^0 production cross sections. These contributions will be classified according to the types of the quarks q and antiquarks \bar{q}' entering the $q\bar{q}'W$ or $q\bar{q}Z$ electroweak vertex. At the Born level, the cross section for production of narrow-width W^\pm and Z^0 bosons in a $q\bar{q}'$ partonic channel is approximately given by

$$\sigma_{q\bar{q}'} \approx \sigma_0 \mathcal{L}_{q\bar{q}'}(\tau) g_{q\bar{q}'} ,$$

| | | W^+ | | | | | W^- | | | | | Z^0 | | | | |
|----------------|----|------------|------------|------------|------------|------------|------------|------------|------------|------------|------------|------------|------------|------------|------------|------------|
| Subprocesses | | $u\bar{d}$ | $u\bar{s}$ | $c\bar{d}$ | $c\bar{s}$ | $c\bar{b}$ | $d\bar{u}$ | $s\bar{u}$ | $d\bar{c}$ | $s\bar{c}$ | $b\bar{c}$ | $u\bar{u}$ | $d\bar{d}$ | $s\bar{s}$ | $c\bar{c}$ | $b\bar{b}$ |
| Tevatron Run-2 | 90 | 2 | 1 | 7 | 0 | | 90 | 2 | 1 | 7 | 0 | 57 | 35 | 5 | 2 | 1 |
| LHC | 74 | 4 | 1 | 21 | 0 | | 67 | 2 | 3 | 28 | 0 | 36 | 34 | 15 | 9 | 6 |

Table I: Partial contributions $\sigma_{q\bar{q}}/\sigma_{tot}$ of quark-antiquark annihilation subprocesses to the total Born cross sections in W^\pm and Z^0 boson production at the Tevatron and LHC (in percent).

where $\tau \equiv Q^2/S$, $Q = M_W$ (M_Z) in W^\pm (Z^0) boson production,

$$\mathcal{L}_{q\bar{q}}(\tau) = \int_\tau^1 \frac{d\xi}{\xi} \left[f_{q/A}(\xi, Q) f_{\bar{q}'/B}(\frac{\tau}{\xi}, Q) + f_{\bar{q}'/A}(\xi, Q) f_{q/B}(\frac{\tau}{\xi}, Q) \right] \quad (12)$$

is the parton luminosity in the $q\bar{q}'$ channel, $g_{q\bar{q}'}$ is the flavor-dependent prefactor, and σ_0 includes the remaining flavor-independent terms [24]. In W^\pm boson production,

$$g_{q\bar{q}'} = V_{q\bar{q}'}^2, \quad (13)$$

where $V_{q\bar{q}'}$ is the appropriate CKM matrix entry. In Z^0 boson production,

$$g_{q\bar{q}'} = \delta_{q\bar{q}'} \left[(1 - 4|e_q| \sin^2 \theta_w)^2 + 1 \right], \quad (14)$$

where $e_q = 2/3$ or $-1/3$ is the quark electric charge in units of the positron charge, and θ_w is the weak mixing angle. The partial cross sections $\sigma_{q\bar{q}'}/\sigma_{tot}$ (where $\sigma_{tot} \equiv \sum_{q,\bar{q}'} \sigma_{q\bar{q}'}$) in the different $q\bar{q}'$ channels are evaluated as $\mathcal{L}_{q\bar{q}'} g_{q\bar{q}'} / \left(\sum_{q,\bar{q}'} \mathcal{L}_{q\bar{q}'} g_{q\bar{q}'} \right)$ and listed in Table I. These values will be modified somewhat by the NLO radiative corrections included in the following subsections.

According to the Table, the contributions of the heavy-quark channels at the Tevatron are small. In W boson production, only 8% of the cross section involves heavy (charm) quarks, while light quarks account for 92%. In Z boson production, heavy quarks contribute even less, with only 3%. Due to the small fractional contribution of the heavy quarks at the Tevatron, the differences between the massive and the massless calculations are negligible given the expected experimental uncertainties.

The LHC probes smaller momentum values x , where the fractional contributions of the initial charm and bottom quarks are much larger. These channels sum up to 22% in W^+ boson production, 31% in W^- boson production, and 15% in Z^0 boson production. Therefore, the following discussion will concentrate on the LHC and only briefly mention the Tevatron processes.

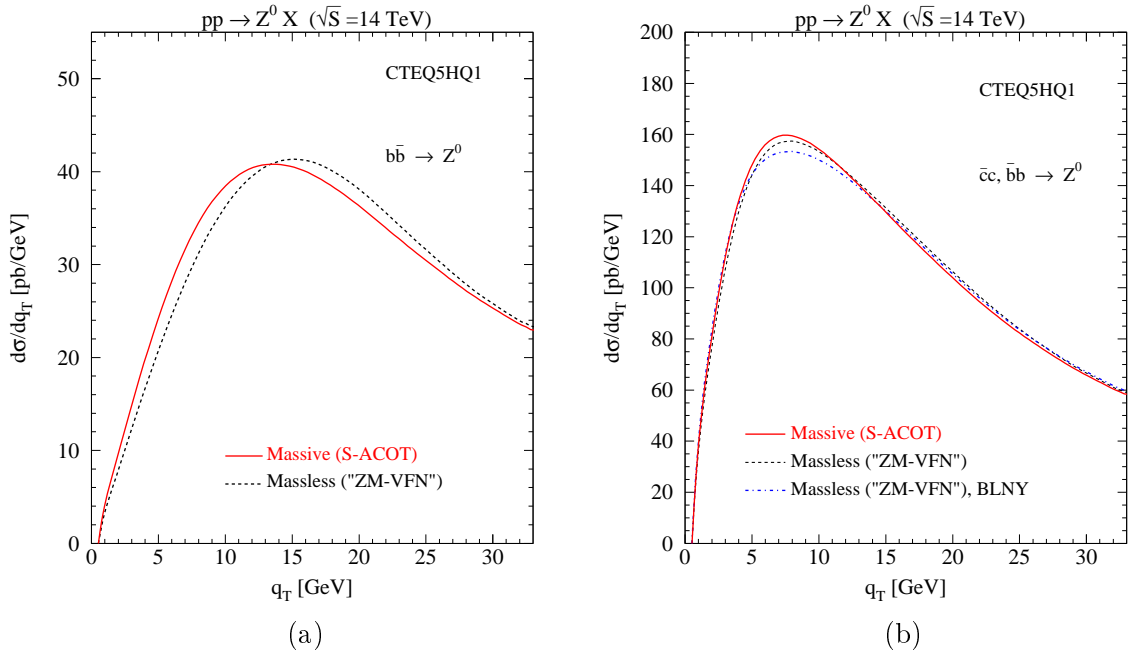


Figure 3: $d\sigma/dq_T$ for $c\bar{c}, b\bar{b} \rightarrow Z^0$ boson production at the LHC: (a) $b\bar{b}$ channel only, (b) combined $c\bar{c}$ and $b\bar{b}$ channels. The solid (red) curve shows the distribution in the massive (S-ACOT) scheme. The dashed (black) curve shows the distribution in the massless (“ZM-VFN”) scheme, computed using the parametrization (11) of the nonperturbative function $\mathcal{F}_{NP}(b, Q)$. The dot-dashed (blue) line was calculated in the “ZM-VFN” scheme using an alternative parameterization [48] of the nonperturbative function $\mathcal{F}_{NP}(b, Q)$.

B. Z^0 boson production at LHC

We first examine the influence of the charm and bottom quark masses on the resummed Z^0 boson cross section at the LHC. Fig. 3 compares the transverse momentum distribution of Z^0 boson production in the heavy-quark ($c\bar{c}$ and $b\bar{b}$) channels at the LHC, calculated in the S-ACOT and “ZM-VFN” schemes. Fig. 3(a) shows the distribution in the $b\bar{b}$ channel only, where the effect is the largest due to the large b quark mass. In the approximate “ZM-VFN” scheme (black dashed line), the $d\sigma/dq_T$ distribution is shifted in the maximum region at ~ 13 GeV to larger transverse momenta by about 2 GeV. This reflects the enhancement of the form factor $b\widetilde{W}(b, Q)$ at $b \sim b_0/m_b \approx 0.25 \text{ GeV}^{-1}$ in the S-ACOT scheme. The region of large transverse momenta ($q_T \gtrsim 25$ GeV) is essentially sensitive only to small impact parameters ($b \lesssim 0.1 \text{ GeV}^{-1}$), where the S-ACOT and ZM-VFN form factors are very close. Consequently, the two schemes give very close predictions in the large- q_T region.

The shift to the larger values of q_T is similar in the $c\bar{c}$ channel, albeit smaller due to the lower charm mass. Fig. 3(b) shows the combined distribution in the $c\bar{c}$ and $b\bar{b}$ channels. The mass-induced shift of the peak of the q_T distribution is much smaller, but clearly visible. One should notice that the distribution of Fig. 3(b) peaks around 7.5 GeV, since it is dominated by the charm contribution, whereas the bottom distribution peaks at 15 GeV (Fig. 3(a)). The combined effect, displayed in Fig. 3(b), is an enhancement of the rate in the peak region of about 2.5%.

For comparison, the dot-dashed (blue) line shows the shift of the “ZM-VFN” q_T distribution due to the choice of a different parameterization for the nonperturbative function $\mathcal{F}_{NP}(b, Q)$ [48]. The difference between the dotted (black) line and the dot-dashed (blue) line provides a conservative estimate of the current experimental uncertainty in $\mathcal{F}_{NP}(b, Q)$. The mass-induced effect is at least comparable to the other uncertainties, when the $c\bar{c}$ and $b\bar{b}$ channels are taken alone. However, these channels cannot be isolated from the light-quark channels in the single-particle inclusive observables. According to Table I, the heavy-quark channels contribute about 15% to the total Z^0 boson cross section. If the light-quark flavors are included, the S-ACOT rate is enhanced in the maximum region by a small value of $\sim 0.3\%$, which is beyond the experimental precision of the LHC.

C. W^\pm boson production at LHC

W^\pm boson production at the LHC is of particular interest, as it will be utilized to measure the W boson mass M_W with high precision (tentatively less than 15 MeV). The W boson mass can be extracted in the leptonic decay $W \rightarrow e\nu$ by fitting the theoretical model for different values of M_W to kinematical Jacobian peaks, arising at $M_T^{e\nu} \approx M_W$ in the leptonic transverse mass ($M_T^{e\nu}$) distribution [56], and at $p_T^e \sim M_W/2 \approx 40$ GeV in the electron p_T^e spectrum.

The S-ACOT and “ZM-VFN” schemes yield essentially identical results for the $M_T^{e\nu}$ distribution, suggesting that the error caused by the massless approximation is likely negligible in the $M_T^{e\nu}$ method. This conclusion follows from the low sensitivity of the $M_T^{e\nu}$ distribution to variations δq_T in the bosonic q_T distributions (suppressed by $\delta q_T^2/M_W^2 \ll 1$). However, the p_T^e distribution may be strongly affected.

To better display percent-level changes in $d\sigma/dp_T^e$ associated with the effects of the heavy

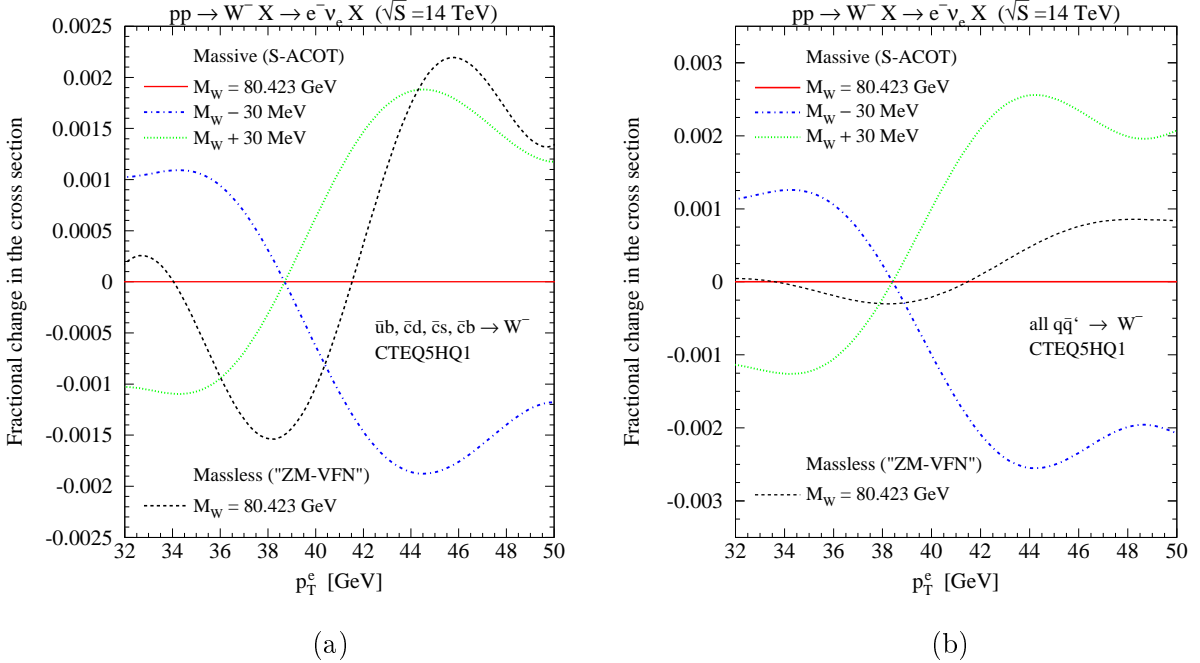


Figure 4: The fractional change in the distribution $d\sigma/dp_T^e$ for $pp \rightarrow W^- X \rightarrow e^- \nu_e X$ at the LHC: a) only partonic channels containing heavy quarks ($\bar{u}b, \bar{c}d, \bar{c}s, \bar{c}b \rightarrow W^-$) are included; (b) all channels are included. The dashed (black) line shows the relative difference between the massless (“ZM-VFN”) and S-ACOT cross sections. The dotted (green) and dot-dashed (blue) lines show the relative changes in the S-ACOT cross section induced by variations of M_W by ± 30 MeV.

quarks, Fig. 4 shows the fractional difference $(d\sigma^{mod}/dp_T^e) / (d\sigma^{S-ACOT}/dp_T^e) - 1$ of the “modified” (e.g. “ZM-VFN”) cross section and the “standard” (S-ACOT) cross section. We compare the modifications due to the approximate massless “ZM-VFN” treatment to the modifications due to explicit variations of M_W in the S-ACOT result.

We first examine the partonic production channels with at least one c or b quark (or their antiparticles) in the initial state. Fig. 4(a) shows the fractional change of the p_T^e distribution for these channels in W^- boson production. The solid red line shows the reference result, calculated using the S-ACOT scheme with $M_W = 80.423$ GeV. The dotted (green) and dot-dashed (blue) lines show the variation of the S-ACOT p_T^e distribution, if the W boson mass is shifted by ± 30 MeV. A small increase of M_W results in a positive shift of the Jacobian peak (dotted green line), which reduces the cross section at $p_T^e < M_W/2$ and increases the cross section at $p_T^e > M_W/2$. Smaller values of M_W result in a shift in the opposite direction.

The dashed black curve is the ratio of the p_T^e distributions calculated in the “ZM-VFN” and S-ACOT schemes for $M_W = 80.423$ GeV. In the heavy-quark channels only (Fig. (4(a))),

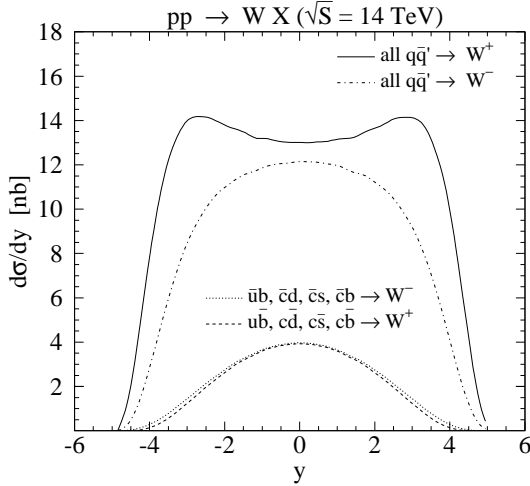


Figure 5: Rapidity distributions of W^\pm bosons at the LHC. The solid (dot-dashed) line is the distribution of the $W^+(W^-)$ bosons in all channels. The dashed (dotted) line is the distribution of the $W^+(W^-)$ bosons in the channels that involve at least one initial-state c or b quark.

the ‘‘ZM-VFN’’ approximation shifts the Jacobian peak in the positive direction. The size of this effect is comparable to a shift in M_W of about +35 MeV.

Fig. 4(a) is also representative of W^+ boson production at the LHC, because the dominant heavy-quark contributions ($c\bar{s} \rightarrow W^+$ and $\bar{c}s \rightarrow W^-$) are charge-conjugated, and the parton density functions of c (s)-quarks and \bar{c} (\bar{s})-anti-quarks are almost identical. Hence, the rates for W^+ and W^- boson production in heavy-quark scattering are very similar.

Fig. 4(b) shows the fractional change in the p_T^e distribution for W^- bosons, summed over all possible partonic states. The total shift of the differential cross section due to the ‘‘ZM-VFN’’ approximation is comparable with a positive M_W shift of about 10 MeV. This value is consistent with the shift of 35 MeV in the c and b channels, in view of the fact that the c, b -channels contribute $\sim 30\%$ to the total W^- cross section according to Table I. The q_T shift is independent of the rapidity y of the W^- boson, because the rapidity distributions of W^- bosons have similar shapes in the heavy-quark and combined channels (see Fig. 5). Consequently the mass-induced shift in the W^- boson q_T distribution is not affected by the rapidity cuts.

We contrast this result with W^+ boson production, where the profile of the rapidity distribution for the heavy-quark channels differs from that for the combined channels. The rapidity distribution of W^+ bosons in all channels (solid line in Fig. 5) has characteristic

shoulders at $y \approx \pm 3$. These shoulders are produced by $u\bar{d}, u\bar{s} \rightarrow W^+$ scattering, enhanced at large momentum fractions x by the valence u -quark distribution. The fraction of c and b channels (dashed line) is the largest at central rapidities, $-1 < y < 1$. In this region, c and b contribute $\sim 29\%$ to the cross section. The difference between the “ZM-VFN” and S-ACOT p_T^e distributions is comparable here to a change in M_W of about 9 MeV. In the full rapidity range, this difference is comparable to $\delta M_W \approx 6$ MeV. If experimental cuts appropriate for the ATLAS experiment ($|y_e| < 2.5$, $p_T^e > 25$ GeV and $\cancel{E}_T > 25$ GeV) are applied, the difference is comparable to $\delta M_W \approx 7.5$ MeV.

The presented estimates may be modified by additional nonperturbative contributions arising in the heavy-quark channels, such as those associated with the “intrinsic” heavy quarks. Our model has neglected such contributions, in view that their magnitude is uncertain, and they are less likely to contribute at the small x typical for W and Z boson production. We assumed that the dominant nonperturbative contribution at $Q \sim M_Z$ ($\approx 70\%$ of $\mathcal{F}_{NP}(b, Q)$) arises from Q dependence of the Sudakov factor, which does not depend on the quark flavor (cf. Section II C). The “ZM-VFN” and S-ACOT functions differ in b space by several tens of percent in the threshold region (cf. Figs. 1 and 2). The extra nonperturbative terms must contribute at a comparable level to be non-negligible. We confirmed this estimate numerically by repeating the analysis of the p_T^e distributions for a varied (rescaled by a factor of two) function $\mathcal{F}_{NP}(b, Q)$ in the heavy-quark channels. The resulting variation in p_T^e distribution for the heavy-quark channels, comparable with δM_W of a few tens MeV (???), is consistent with the effect of the rescaling of $\mathcal{F}_{NP}(b, Q)$ in b space, of order of the difference of the “ZM-VFN” and S-ACOT form factors $\widetilde{W}(b, Q)$ in the large- b region.

D. Z^0 and W^\pm boson production at the Tevatron

The dependence on the heavy-quark masses in W^\pm and Z^0 boson production at the Tevatron follows nearly the same pattern as that at the LHC. In Z^0 boson production via c and b quark channels at the Tevatron, the q_T distribution in the “ZM-VFN” approximation is shifted toward larger q_T with respect to the S-ACOT distribution, in analogy to the similar shift at the LHC (cf. Fig. 3). The maximum of the q_T distribution in the $b\bar{b}$ channel is shifted by approximately 2.5 GeV if the masses of the quarks are neglected; this is slightly larger

than the shift at the LHC. However, modifications in the q_T distribution in the combined initial-state channels are negligible, because c and b scattering contributes only 3% to the total Z^0 cross section (cf. Table I).

The analysis of W boson production at the Tevatron is less involved, given that the rates for the processes $p\bar{p} \rightarrow W^+X$ and $p\bar{p} \rightarrow W^-X$ are related by charge conjugation. The electron p_T^e distributions in the c and b quark channels at the Tevatron qualitatively follow the pattern shown in Fig. 4(a) for the LHC. The difference between the p_T^e distributions in the “ZM-VFN” and S-ACOT schemes at the Tevatron is comparable to the effect of a M_W increase by 45 MeV (vs. 35 MeV at the LHC). The heavy-quark channels contribute just 8% to the total W^\pm cross section at the Tevatron. Consequently the net M_W shift in all channels (3 MeV in the p_T^e method and 0 in the $M_T^{e\nu}$ method) is tiny compared to the expected experimental uncertainty of $\sim 30 - 40$ MeV.

E. Higgs boson production

In light of our analysis of the $b\bar{b} \rightarrow Z^0$ channel (Sec. III B), we anticipate that production of Higgs bosons H^0 via $b\bar{b}$ annihilation is also sensitive to the heavy-quark mass effects. In the standard model, the gluon-gluon fusion process $gg \rightarrow H^0$ is the dominant production channel for a wide range of Higgs boson masses at both the Tevatron and LHC (see, e.g., [3, 4, 5] and references therein). Following the gluon-gluon fusion, the next most important channels at the Tevatron are associated WH^0 and ZH^0 production, and vector boson fusion. At the LHC, the next largest production modes are the electroweak boson fusion and Higgs-strahlung processes. The process $b\bar{b} \rightarrow H^0$ typically contributes less than 1% of the total production cross section. In view of the current uncertainty in the Higgs transverse momentum distribution [57], effects due to the heavy quark mass in the $b\bar{b}$ channel will be negligible in the standard model.

The question becomes more interesting in extensions of the standard model containing two Higgs doublets, like the minimal supersymmetric standard model (MSSM), where the Yukawa couplings of the bottom quarks to the neutral Higgs bosons h^0 , H^0 and A^0 depend on the supersymmetric parameter $\tan\beta$. If $\tan\beta$ is large, the bottom Yukawa coupling is strongly enhanced, while the top quark Yukawa coupling remains nearly constant or is suppressed (see Ref. [4]). The $b\bar{b}$ annihilation rate is comparable to the gluon-gluon fusion

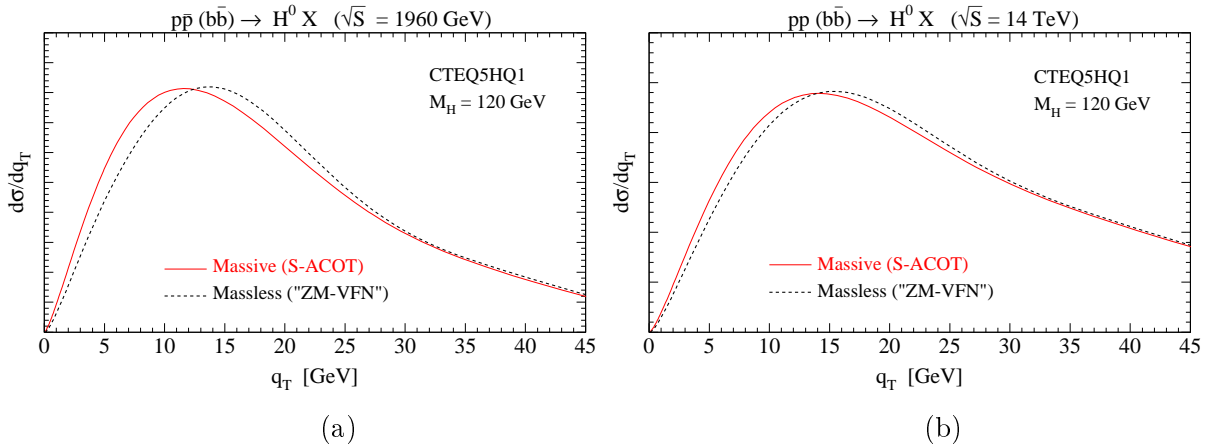


Figure 6: Transverse momentum distribution of on-shell Higgs bosons in the $b\bar{b} \rightarrow H^0$ channel at (a) the Tevatron and (b) LHC. The solid (red) lines show the q_T distribution in the massive (S-ACOT) scheme. The dashed (black) lines show the distribution in the massless (“ZM-VFN”) scheme.

rate for medium values of $\tan\beta$ and can dominate the cross section for $\tan\beta \gtrsim 30$.

We implemented the heavy-quark mass effects in the resummation subroutine for $b\bar{b} \rightarrow H^0$ developed in an earlier study [58].¹ Fig. 6 displays $d\sigma/dq_T$ for $b\bar{b} \rightarrow H^0$ boson production at (a) the Tevatron and (b) LHC. The Higgs boson mass is chosen to be $M_H = 120$ GeV. The supersymmetric $b\bar{b}$ – Higgs couplings are obtained at leading order by rescaling the standard model coupling: $g_{b\bar{b}\{h^0, H^0, A^0\}}^{MSSM} = \{-\sin\alpha, \cos\alpha, \sin\beta\gamma_5\}g_{b\bar{b}H}^{SM}/\cos\beta$ [59, 60]. The net effect of the bottom quark masses on q_T distributions will be the same for both SM and MSSM neutral Higgs bosons, up to an overall normalization constant. For this reason, Fig. 6 does not specify the overall normalization of q_T distributions.

The S-ACOT and “ZM-VFN” distributions $d\sigma/dq_T$ are shown by the solid (red) and dashed (black) lines, respectively. A significant shift of the distribution to larger values of q_T is seen in the “ZM-VFN” approximation. As in $b\bar{b} \rightarrow Z^0$ process (Sec. III B), the enhancement of the q_T distribution at small q_T is caused by the enhancement in the S-ACOT form factor $b\widetilde{W}(b, Q)$ at intermediate and large b ($b > 0.1 \text{ GeV}^{-1}$). At the Tevatron, Fig. 6(a), the q_T maximum shifts in the “ZM-VFN” approximation to larger q_T by about 2 GeV out of 11.7 GeV (about 17%). For a Higgs mass $M_H = 200$ GeV, the maximum of

¹ We thank A. Belyaev and C.-P. Yuan for pointing out a typo in the $\mathcal{C}_{q/q}$ function in Ref. [58], which does not affect the results shown in this section.

Differences in $d\sigma/dq_T$ for $b\bar{b} \rightarrow H^0$ at the LHC

| m_H [GeV] | | 120 | 250 | 600 |
|-----------------------------------|--------------------|--------------|--------------|--------------|
| Position of the maximum [GeV] | “ZM-VFN” S-ACOT | 15.4 14.1 | 16.8 15.8 | 18.8 18.2 |
| Difference in the positions [GeV] | | 1.3 | 1.0 | 0.6 |

Table II: Positions of the maximum of the distribution $d\sigma/dq_T$ in $b\bar{b} \rightarrow H^0$ process at the LHC in the mass-dependent (S-ACOT) and massless (“ZM-VFN”) calculations, as well as the differences of these positions.

$d\sigma/dq_T$ shifts by about 1.9 GeV out of 12.7 GeV.

The corresponding q_T distributions for the LHC are shown in Fig. 6(b). The difference between the “ZM-VFN” and S-ACOT calculations is smaller compared to the Tevatron, because the influence of the region $b > 0.1 \text{ GeV}^{-1}$ is reduced at smaller momentum fractions x probed at the LHC [49]. The maximum of the transverse momentum distribution shifts in the “ZM-VFN” approximation by about 1.3 GeV (9% out of 14.1 GeV) to larger q_T . The results for two other Higgs masses ($M_H = 250$ and 600 GeV) are summarized in Table II. The full q_T dependence of the $b\bar{b} \rightarrow H$ process is affected by additional factors, such as the constraints on phase space available for QCD radiation (less relevant at small q_T). The full q_T dependence is investigated elsewhere [61].

IV. CONCLUSION

In the present paper, we make use of recent theoretical developments to estimate the impact of heavy-quark masses m_Q on transverse momentum (q_T) distributions in production of W , Z , and Higgs bosons at the Tevatron and LHC. We note that the the zero-mass (“massless”) variable flavor number scheme is not consistent in the heavy-quark channels, if q_T is of order of the heavy-quark mass m_Q . To properly assess the m_Q dependence, we perform resummation of the large logarithms $\ln(q_T^2/Q^2)$ in the Collins-Soper-Sterman approach, formulated in a general variable flavor number factorization scheme (S-ACOT scheme) to correctly resum the collinear logarithms $\ln(\mu_F/m_Q)$.

We compare our consistent treatment of the heavy-quark mass dependence with an approach based on the ZM-VFN scheme. The proper treatment of the heavy-quark masses leads to an enhancement of the form factor $\widetilde{W}(b, Q)$ at intermediate and large impact parameters, which in turn increases the transverse momentum distribution at small q_T . In Drell-Yan production of heavy bosons, the cumulative effect in the S-ACOT scheme shifts the peak of the $d\sigma/dq_T$ distribution to smaller values of q_T . The mass effects are negligible if q_T is of order Q .

The mass dependence is magnified in subprocesses dominated by scattering of initial-state bottom quarks, as a consequence of the larger b -quark mass. In the production of Z^0 and light Higgs bosons via $b\bar{b}$ annihilation at the LHC, the maximum of $d\sigma/dq_T$ shifts from $13.5 - 14$ GeV in the S-ACOT scheme to ≈ 15 GeV in the “ZM-VFN” approximation. At the Tevatron, the maximum shifts from ≈ 10 to 12 GeV. Our computation is applied to single-particle inclusive production, when no heavy quarks are observed in the final state. Since the single-particle inclusive cross sections receive contributions from both the heavy-quark channels and intensive light-quark channels, the m_Q dependence is reduced below the experimental sensitivity in several cases, notably in W^\pm and Z^0 boson production at the Tevatron, and Z^0 boson production at the LHC. On the other hand, the signal from the heavy-quark channels may be enhanced by tagging one or two heavy quarks in the final state. In that case, mass-dependent effects of a similar magnitude may be observed in some regions of phase space, *e.g.*, at small q_T of the boson-heavy quark system.

Since the LHC plans to measure the W boson mass M_W to a high precision, we must fully account for all potential uncertainties, including the heavy-quark mass effects. At the LHC, the massless “ZM-VFN” approximation introduces a bias in the measurement of M_W from the transverse momentum distribution $d\sigma/dp_T^e$ of the electrons, comparable to a positive M_W shift by ~ 10 MeV. In W^+ boson production the bias is comparable to the M_W shift of 9 MeV at central rapidities of W bosons ($|y| \leq 1$) and 6 MeV in the whole rapidity range. These effects are not negligible in view of the desired precision of the M_W measurement of ~ 15 MeV.

Acknowledgments

We thank A. Belyaev and C.-P. Yuan for valuable discussions. An independent study [61] of the resummation in the $b\bar{b} \rightarrow$ Higgs process, including the heavy-quark mass effects, has been brought to our attention as we completed this paper. We also thank U. Baur and S. Heinemeyer for helpful communications. F.I.O. and S.B. acknowledge the hospitality of Fermilab and BNL, where a portion of this work was performed. The work of S. B. and F. I. O. was partially supported by the U.S. Department of Energy under grant DE-FG03-95ER40908 and the Lightner-Sams Foundation. The work of P. M. N. was supported in part by the U.S. Department of Energy, High Energy Physics Division, under Contract W-31-109-ENG-38.

- [1] R. Brock et al. (1999), hep-ex/0011009.
- [2] S. Haywood et al. (1999), hep-ph/0003275.
- [3] M. Carena and H. E. Haber, *Prog. Part. Nucl. Phys.* **50**, 63 (2003).
- [4] M. Spira, *Fortsch. Phys.* **46**, 203 (1998).
- [5] K. A. Assamagan et al. (Higgs Working Group) (2004), hep-ph/0406152.
- [6] M. Gluck, E. Hoffmann, and E. Reya, *Z. Phys.* **C13**, 119 (1982).
- [7] M. Gluck, R. M. Godbole, and E. Reya, *Z. Phys.* **C38**, 441 (1988), Erratum: *ibid.*, **C39**, 590 (1988).
- [8] P. Nason, S. Dawson, and R. K. Ellis, *Nucl. Phys.* **B327**, 49 (1989), Erratum: *ibid.*, **B335**, 260 (1990).
- [9] E. Laenen, S. Riemersma, J. Smith, and W. L. van Neerven, *Phys. Lett.* **B291**, 325 (1992).
- [10] E. Laenen, S. Riemersma, J. Smith, and W. L. van Neerven, *Nucl. Phys.* **B392**, 162 (1993).
- [11] E. Laenen, S. Riemersma, J. Smith, and W. L. van Neerven, *Nucl. Phys.* **B392**, 229 (1993).
- [12] R. V. Harlander and W. B. Kilgore, *Phys. Rev.* **D68**, 013001 (2003).
- [13] J. Campbell, R. K. Ellis, F. Maltoni, and S. Willenbrock, *Phys. Rev.* **D67**, 095002 (2003).
- [14] F. Maltoni, Z. Sullivan, and S. Willenbrock, *Phys. Rev.* **D67**, 093005 (2003).
- [15] S. Dawson, C. B. Jackson, L. Reina, and D. Wackerlo, *Phys. Rev.* **D69**, 074027 (2004).
- [16] S. Dawson, C. B. Jackson, L. Reina, and D. Wackerlo, *Phys. Rev. Lett.* **94**, 031802 (2005).

- [17] S. Dawson, C. B. Jackson, L. Reina, and D. Wackerlo (2005), hep-ph/0508293.
- [18] S. Dittmaier, M. Kramer, and M. Spira, Phys. Rev. **D70**, 074010 (2004).
- [19] J. Campbell, R. K. Ellis, F. Maltoni, and S. Willenbrock, Phys. Rev. **D69**, 074021 (2004).
- [20] F. Maltoni, T. McElmurry, and S. Willenbrock (2005), hep-ph/0505014.
- [21] Y. L. Dokshitzer, D. Diakonov, and S. I. Troian, Phys. Lett. **B78**, 290 (1978).
- [22] G. Parisi and R. Petronzio, Nucl. Phys. **B154**, 427 (1979).
- [23] G. Altarelli, R. K. Ellis, M. Greco, and G. Martinelli, Nucl. Phys. **B246**, 12 (1984).
- [24] J. C. Collins, D. E. Soper, and G. Sterman, Nucl. Phys. **B250**, 199 (1985).
- [25] R. K. Ellis and S. Veseli, Nucl. Phys. **B511**, 649 (1998).
- [26] A. Kulesza, G. Sterman, and W. Vogelsang, Phys. Rev. **D66**, 014011 (2002).
- [27] X. Ji, J.-P. Ma, and F. Yuan, Phys. Lett. **B597**, 299 (2004).
- [28] P. M. Nadolsky, N. Kidonakis, F. I. Olness, and C.-P. Yuan, Phys. Rev. **D67**, 074015 (2003).
- [29] J. C. Collins, Phys. Rev. **D58**, 094002 (1998).
- [30] M. A. G. Aivazis, J. C. Collins, F. I. Olness, and W.-K. Tung, Phys. Rev. **D50**, 3102 (1994).
- [31] B. A. Kniehl, M. Kramer, G. Kramer, and M. Spira, Phys. Lett. **B356**, 539 (1995).
- [32] M. Buza, Y. Matiounine, J. Smith, and W. L. van Neerven, Eur. Phys. J. **C1**, 301 (1998).
- [33] R. S. Thorne and R. G. Roberts, Phys. Rev. **D57**, 6871 (1998).
- [34] R. S. Thorne and R. G. Roberts, Phys. Lett. **B421**, 303 (1998).
- [35] M. Cacciari, M. Greco, and P. Nason, JHEP **05**, 007 (1998).
- [36] A. Chuvakin, J. Smith, and W. L. van Neerven, Phys. Rev. **D61**, 096004 (2000).
- [37] M. Kramer, F. I. Olness, and D. E. Soper, Phys. Rev. **D62**, 096007 (2000).
- [38] W.-K. Tung, S. Kretzer, and C. Schmidt, J. Phys. **G28**, 983 (2002), hep-ph/0110247.
- [39] S. J. Brodsky, P. Hoyer, C. Peterson, and N. Sakai, Phys. Lett. **B93**, 451 (1980).
- [40] M. Abramowitz and I. Stegun, eds., *Handbook of mathematical functions* (Dover Publications, Inc., New York, N. Y., 1972), chap. 9.6.
- [41] J. C. Collins and D. E. Soper, Nucl. Phys. **B194**, 445 (1982).
- [42] C. T. H. Davies, B. R. Webber, and W. J. Stirling, Nucl. Phys. **B256**, 413 (1985).
- [43] G. A. Ladinsky and C.-P. Yuan, Phys. Rev. **D50**, 4239 (1994).
- [44] R. K. Ellis, D. A. Ross, and S. Veseli, Nucl. Phys. **B503**, 309 (1997).
- [45] F. Landry, R. Brock, G. Ladinsky, and C.-P. Yuan, Phys. Rev. **D63**, 013004 (2001).
- [46] A. Guffanti and G. E. Smye, JHEP **10**, 025 (2000).

- [47] A. Kulesza and W. J. Stirling, Eur. Phys. J. **C20**, 349 (2001).
- [48] F. Landry, R. Brock, P. M. Nadolsky, and C.-P. Yuan, Phys. Rev. **D67**, 073016 (2003).
- [49] J. Qiu and X. Zhang, Phys. Rev. **D63**, 114011 (2001).
- [50] A. V. Konychev and P. M. Nadolsky (2005).
- [51] J. C. Collins and D. E. Soper, Nucl. Phys. **B197**, 446 (1982).
- [52] G. P. Korchemsky and G. Sterman, Nucl. Phys. **B555**, 335 (1999).
- [53] S. Tafat, JHEP **05**, 004 (2001).
- [54] H. L. Lai et al. (CTEQ Collaboration), Eur. Phys. J. **C12**, 375 (2000).
- [55] C. Balazs and C.-P. Yuan, Phys. Rev. **D56**, 5558 (1997).
- [56] J. Smith, W. L. van Neerven, and J. A. M. Vermaseren, Phys. Rev. Lett. **50**, 1738 (1983).
- [57] M. Dobbs et al. (2004), hep-ph/0403100.
- [58] C. Balazs, H.-J. He, and C. P. Yuan, Phys. Rev. **D60**, 114001 (1999).
- [59] J. F. Gunion and H. E. Haber, Nucl. Phys. **B272**, 1 (1986), Erratum: *ibid.*, **B402**, 567 (1993).
- [60] J. F. Gunion, H. E. Haber, G. L. Kane, and S. Dawson, eds., *The Higgs Hunter's Guide* (SCIPP-89/13; Errata hep-ph/9302272).
- [61] A. Belyaev, P. Nadolsky, and C.-P. Yuan, in preparation.